Journal of Physics: Conference Series **174** (2009) 012037 doi:10.1088/1742-6596/174/1/012037

Noise stabilization effects in models of interdisciplinary physics

B Spagnolo[1], G Augello[1], P Caldara[1], A Fiasconaro[1], A La Cognata[1], N Pizzolato[1], D Valenti[1], A A Dubkov[2] and A L Pankratov[3]

[1]Dipartimento di Fisica e Tecnologie Relative, Group of Interdisciplinary Physics[1], Università di Palermo,
Viale delle Scienze, pad. 18, I-90128 Palermo, Italy
[2]Radiophysical Department, N. Novgorod State University,
Gagarin ave.23, Nizhniy Novgorod, 603950 Russia
[3]Institute for Physics of Microstructures of RAS, GSP-105, 603950 Nizhny Novgorod, Russia

E-mail: spagnolo@unipa.it

Abstract. Metastability is a generic feature of many nonlinear systems, and the problem of the lifetime of metastable states involves fundamental aspects of nonequilibrium statistical mechanics. The investigation of noise-induced phenomena in far from equilibrium systems is one of the approaches used to understand the behaviour of physical and biological complex systems. The enhancement of the lifetime of metastable states through the noise enhanced stability effect and the role played by the resonant activation phenomenon will be discussed in models of interdisciplinary physics: (i) polymer translocation dynamics; (ii) transient regime of FitzHugh-Nagumo model; (iii) market stability in a nonlinear Heston model; (iv) dynamics of Josephson junctions; (v) metastability in a quantum bistable system.

1. Introduction

Relaxation in many natural systems proceeds through metastable states, often observed in condensed matter physics, in cosmology, biology and high-energy physics. In spite of such ubiquity, the microscopic understanding of metastability still raises fundamental questions. This is because we are dealing with a typical out of equilibrium statistical dynamical phenomenon. A physical quantity which characterize the stability of a metastable state is the mean first passage time, which gives a measure of the lifetime of the metastable state. The dependence of the lifetime on the noise intensity for metastable and unstable systems was revealed to have resonance character. Typical examples are the resonant activation (RA) phenomenon [1]-[3] and the noise enhanced stability (NES) [4]. This resonance-like phenomenon shows that the noise can modify the stability of the system in a counterintuitive way: the system remains in the metastable state for a longer time than in the deterministic case [4]-[12]. In this paper we will shortly review the enhancement of the lifetime of metastable states and the role played by the resonant activation phenomenon in models of interdisciplinary physics: (i) polymer translocation dynamics; (ii) transient regime of FitzHugh-Nagumo model; (iii) market stability in a nonlinear Heston model; (iv) dynamics of Josephson junctions; (v) metastability in a quantum bistable system.

[1] Electronic address: http://gip.dft.unipa.it

2. Polymer translocation dynamics

The study of the dynamics of translocation of individual polymers across nanometer-scale pores is essential to help the understanding of how biological systems work. In a fundamental work on polymer translocation [13], it was demonstrated that the crossing time of single-stranded DNA molecules, forced by an applied electric field to move through a $2.6 - nm$ diameter ion channel, linearly increases with the polymer length. By using a similar experimental setup, Meller *et al.* [14] have also shown that the time-length relationship depends on specific interactions between the DNA and the nanopore walls. Very interesting experimental results by Han *et al.* [15] show longer crossing times for shorter DNA molecules, suggesting the existence of a quasi-equilibrium state of the polymer after being trapped for a time. This work suggests that, in same cases, a special condition for the polymer travelling across a nanometer-scale channel can be realized to make it temporarily trapped into a metastable state. In this framework, our investigations on the dynamics of polymers under the influence of a noisy environment show the presence of the noise enhanced stability (NES) effect [4]-[12] for short polymers escaping from a potential barrier. We also show how thermal fluctuations influence the motion of short chain molecules, by inducing two different regimes of translocation in the transport dynamics, depending on the length of the polymer.

2.1. Model and dynamics simulations

The polymer is modeled by a semi-flexible chain of N beads connected by harmonic springs according the Rouse model [16]. The van der Waals interactions between all beads are kept into account by introducing a Lennard-Jones potential. We neglect any hydrodynamic effect and volume effect. In order to confer a suitable stiffness to the chain, a bending recoil torque is included in the model, with a rest angle $\theta_0 = 0$ between two consecutive bonds. The potential energy of the modeled chain molecule is

$$U = U_{\rm Har} + U_{\rm Bend} + U_{\rm LJ}, \tag{1}$$

where $U_{\rm Har} = \sum_{i=1}^{N-1} K_{\rm r}(r_{i,i+1} - d)^2$ represents the energy required to extend the bond between two consecutive beads, $U_{\rm Bend} = \sum_{i=2}^{N-1} K_\theta(\theta_{i-1,i+1} - \theta_0)^2$ the work required to bend the chain, and $U_{\rm LJ} = 4\epsilon_{\rm LJ} \sum_{i,j(i\neq j)} \left[\left(\frac{\sigma}{r_{ij}}\right)^{12} - \left(\frac{\sigma}{r_{ij}}\right)^{6} \right]$ the Lennard-Jones potential. Here $K_{\rm r}$ is the elastic constant, r_{ij} the distance between particles i and j, K_θ the bending modulus, $\epsilon_{\rm LJ}$ the LJ energy depth and σ the monomer diameter. The polymer motion is modeled in a two-dimensional domain as a stochastic process of diffusion in the presence of a potential barrier having the form

$$U_{\rm Ext}(x) = ax^2 - bx^3, \tag{2}$$

with parameters $a = 3 \cdot 10^{-3}$ and $b = 2 \cdot 10^{-4}$. The drift of the $i^{\rm th}$ monomer of the chain molecule is described by the following overdamped Langevin equations

$$\gamma \frac{dx}{dt} = -\frac{\partial U}{\partial x} - \frac{\partial U_{\rm Ext}(x)}{\partial x} + \sqrt{D}\xi_{\rm x}(t), \tag{3}$$

$$\gamma \frac{dy}{dt} = -\frac{\partial U}{\partial y} + \sqrt{D}\xi_{\rm y}(t), \tag{4}$$

where U is the interaction potential, defined by Eq. (1), $\xi_x(t)$ and $\xi_y(t)$ are white Gaussian noise modeling the temperature fluctuations, with the usual statistical properties, namely $\langle \xi_k(t) \rangle = 0$ and $\langle \xi_k(t)\xi_l(t+\tau) \rangle = D\delta_{(k,l)}\delta(\tau)$ for $(k, l = x, y)$ and γ is the friction coefficient. In this work we set the γ parameter equal to one. Our simulation time t_s is scaled with the friction parameter as $t_s = t/\gamma$, therefore we use arbitrary units for all computed translocation times. We set both $K_{\rm r}$ and K_θ equal to 10, $\epsilon_{\rm LJ}$ equal to 0.1 and σ equal to 3, in arbitrary units. The inter-beads rest length d is chosen equal to 5, while the number of monomers N ranges from 2 to 40 units.

2.2. Results and conclusions

First results concern the case of harmonic potential forces U_{Har}, the cubic potential of Eq. (2) and initial unstable conditions. We find the noise enhanced stability (NES) effect for a short polymer escaping from a potential barrier [16]. In Fig. 1a we show how the MFPT changes with the noise intensity at different polymer lengths. Assuming identical unstable initial conditions, we find that the NES effect is more relevant for shorter chains (lower number of monomers). The maximum of the MFPT rapidly decreases at increasing polymer length and its position shifts towards higher levels of noise. The dynamics of shorter chains is much more similar to that of

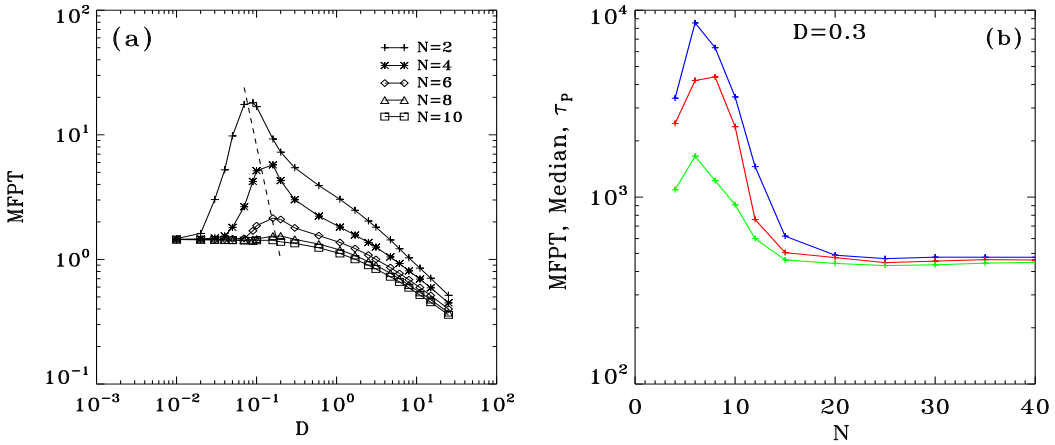

Figure 1. (a) Mean first passage time vs. noise intensity for five different numbers N of monomers in the polymer. The initial unstable condition $x_0 = 1.3$ is the same for all the monomers. The dashed line indicate the shift of the maximum of the MFPT. (b) Mean first passage time (blue line), median of the crossing time distribution (red line) and most probable translocation time (green line) vs. polymer length (number of beads) for noise intensity $D = 0.3$.

a single particle escaping from the potential well. As a consequence shorter chains show more pronounced NES effect, with higher maximum values of the MFPT. On the other hand, longer polymers need higher noise intensity values to move the center of mass back into the metastable state, starting from initial unstable states.

Now we consider all the potential energies reported in Eq. (1) and the polymer initially placed in the metastable state [17]. The different dynamics of translocation of short and long polymers is investigated as a function of the noise intensity. The results are reported in Fig. 1b. We report the MFPT, the median and the mode (τ_p) of the polymer translocation time distribution as a function of the chain length, for a noise intensity $D = 0.3$. Two different regimes of translocation are clearly present: for $N \leq 15$ all characteristic times show a maximum at $N \simeq 7$, while for $N \geq 15$ a common plateau is observed. This maximum is more evident in the MFPT than in τ_p, but the height of both peaks is rapidly reduced when the noise intensity increases. This maximum occurs at a polymer length corresponding to the persistence length of the chain L_p, which represents the length over which the correlations in the direction of the tangent to the polymer are lost. Experimental and theoretical studies on the translocation time, taken by a chain molecule to cross a membrane, show a strong dependence of this time with the length of the polymer. In this work we propose a possible reason of this dependence. After been trapped for a while, the molecule leaves the top of the barrier exhibiting an enhancement of the mean crossing time as a function of the temperature fluctuations. This is a typical signature of the presence of a metastable state in the system investigated. Our simulations demonstrate that longer polymers can travel the same channel distance faster than shorter chains. This result is in agreement with the experimental measurements of DNA mobility carried out by Han *et al.* [15],

but a deeper analysis on the role of initial conditions on the translocation time is necessary.

3. FitzHugh-Nagumo model with external noise

In this section we study the dynamics of a neuron considered as an open system perturbed by periodic deterministic forcing and random fluctuations of environmental parameters. We analyze the stochastic dynamics of a neuron described by the FitzHugh-Nagumo (FHN) model

$$\dot{x} = x - \frac{x^3}{3} - y + A sin(\omega t + \varphi_0) + \zeta_x, \quad (5)$$

$$\dot{y} = \epsilon(x + I), \quad (6)$$

where x is the membrane potential, characterized by a fast dynamics, and y is the recovery variable, which exhibits a slow dynamics responsible for the refractory behaviour of the neuron. In Eq. (5), A and ω are respectively amplitude and frequency of the external forcing, $\zeta_x(t)$ is a self-correlated noise described by the Ornstein-Uhlenbeck process [18]

$$\frac{d\zeta_x(t)}{dt} = -\frac{1}{\tau}\zeta_x(t) + \frac{1}{\tau}\xi_x(t), \quad (7)$$

with τ correlation time of the colored noise, $\xi_x(t)$ Gaussian white noise with zero mean and correlation function $< \xi_x(t)\xi_x(t') >= \sigma_x\,\delta(t - t')$, and σ_x noise intensity. A self-correlated noise is more suitable than white noise to represent the random fluctuations in real systems, where the noise spectrum is characterized by the presence of a cut-off. The correlation function of the noise source is $\langle \zeta_x(t)\zeta_x(t') \rangle = \frac{\sigma_x}{2\tau} e^{-|t-t'|/\tau}$.

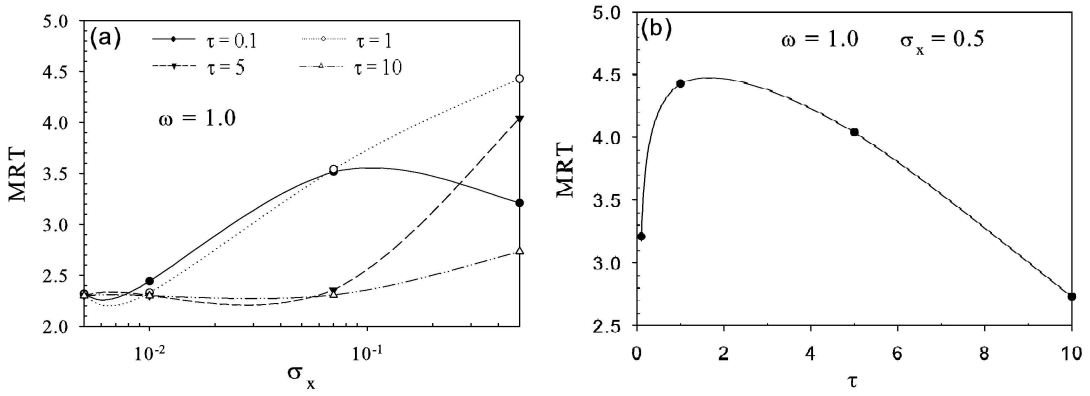

Figure 2. (a) Nonmonotonic behaviour (with a maximum) of MRT as a function of the noise intensity σ_x, for $\omega = 1.0$: in the presence of colored noise this effect disappears as correlation time increases. (b) Nonmonotonic behaviour of the MRT as a function of the correlation time τ, for $\omega = 1.0$ and $\sigma_x = 0.5$. The values of the parameters are: $I = 1.1$, $\epsilon = 0.05$, $\varphi_0 = 0$, $A = 0.5$. The initial state is (x_0, y_0), with $x_0 = -I$, $y_0 = -I + I^3/3$.

In a previous work the system response has been studied, under the influence of a periodic driving signal, as a function of the white noise intensity [19]. The authors showed the occurrence of resonant activation (RA) and noise enhanced stability (NES). The presence of random fluctuations produces modifications in the resonant activation (RA) phenomenon observed in deterministic regime and causes noise enhanced stability to appear in the minimum of RA. NES effect and modifications in RA are connected with the appearance of neuron excitability even if A and ω take values in the deterministic no-firing region. This indicates that noise, because

of its cooperative action with the periodic force, can induce neuron excitability, also when, in deterministic regime, the firing is prohibited due to the parameter values.

In order to study the dynamics of the FHN system we introduce the mean response time defined as $< T >= 1/N \sum_{i=1}^{N} T_i$, with T_i the *first response time*, that is, the time for which the first spike occurs. We analyze the behaviour of the mean response time (MRT) of the neuron, in the presence of periodical stimulus, as a function of the noise intensity. The results, shown in Fig. 2a, evidence the presence of a noise enhanced stability (NES) phenomenon. In particular, MRT shows a nonmonotonic behavior as a function of σ_x (see panel a): starting from $\sigma_x = 0.005$, for intermediate levels of noise intensity an increase of MRT appears. For higher noise intensities a decrease of MRT is observed. We note that the strong dependence of MRT on the noise intensity is suppressed as correlation time increases. Finally, we study MRT as a function of the correlation time τ. The results, shown in Fig. 2b, indicate the presence of a nonmonotonic behaviour of MRT as a function of τ for a fixed value of noise intensity ($\sigma_x = 0.5$), confirming that high values of the correlation time cause the suppression of the noise effects on MRT.

4. A market model with stochastic volatility

Econophysics is a new interdisciplinary research field appeared and developed during last years. Theories and methods, originally developed by physicists in statistical physics to study complex systems, are applied to analyse financial market data [20, 21]. A big amount of work has been addressed to the empirical investigation of different phenomena to find universal laws underlying the dynamics of financial market. During last decades, a considerable effort has been devoted to the construction of models to reproduce and predict the behavior of real market, where the stock option evolution is determined by many traders interacting with each other and using different strategy to increase their own profit. Arbitrariness and nonlinearity present in the system lead to regard the financial market as a complex system where the randomness of the human behavior can be modelled by using stochastic processes. A common approach, used to describe the evolution of stock prices, is based on the Heston model. In this context, empirical verification with stocks and options showed good agreement with real data [22]. A further investigation on the Heston model has been recently performed [23]-[27]. This model consists of two coupled stochastic differential equations which represent the log-normal geometric Brownian motion stock process and the Cox-Ingersoll-Ross (CIR) mean-reverting stochastic process [24]. By using the *log* of the price, $x(t) = ln\ p(t)$, a generalization of the Heston model has been proposed to take into account feedback effects responsible for price fluctuations. Here, a cubic nonlinearity is introduced to consider the different dynamical regimes by the motion of a fictitious "Brownian particle" moving in an effective potential with a metastable state. This nonlinear Heston (NLH) model is defined by the following equations

$$dx(t) = -\left(\frac{\partial U}{\partial x} + \frac{v(t)}{2}\right) dt + \sqrt{v(t)} dW_1(t) \tag{8}$$

$$dv(t) = a(b - v(t))dt + c\sqrt{v(t)} dW_2(t), \tag{9}$$

where $U(x) = 2x^3 + 3x^2$ is the *effective* cubic potential with a metastable state at $x_{me} = 0$, a maximum at $x_m = -1$, and a cross point between the potential and the x axes at $x_c = -1.5$. $W_1(t)$ and $W_2(t)$ are uncorrelated Wiener processes with the usual statistical properties $< dW_i >= 0$, $< dW_i(t) dW_j(t') >= dt\ \delta(t - t')\ \delta_{i,j}$ $(i, j = 1, 2)$. Here, v is the CIR process, which is defined by three parameters, b, a and c. They represent respectively the long term variance, the rate of mean reversion to the long term variance, and the volatility of variance, often called the *volatility of volatility*. The stochastic volatility $v(t)$ is characterized by exponential autocorrelation and *volatility clustering* [21, 26], that is alternating calm with burst

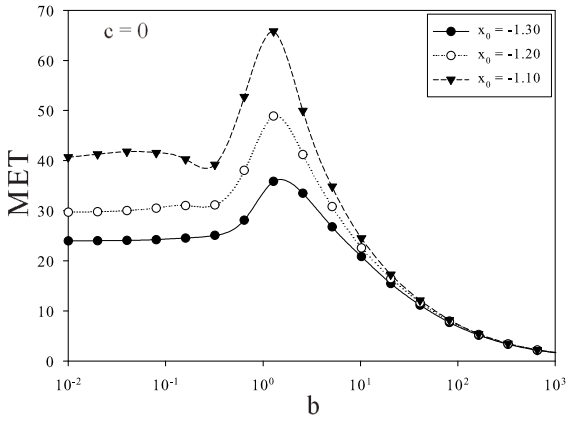

Figure 3. Mean escape time (MET) for 3 different unstable starting positions, when only the reverting term is present: $a = 10^{-2}$, $c = 0$. The curves are averaged over 10^5 escape events.

periods of volatility. The average exit time of the system from the stable to the unstable domain of the metastable potential $U(x)$ may be prolonged by imposing external noise: this phenomenon is named noise enhanced stability (NES). The NES effect and its different dynamical regimes can be explained considering the barrier "*seen*" by the Brownian particle starting at the initial position x_0, that is $\Delta U_{in} = U(x_{max}) - U(x_0)$, and by comparing it with the height of the barrier ΔU characterizing the metastable state [6, 9]. By investigating the mean escape time (MET), as a function of the model parameters a, b and c, we find the parameter region where a nonmonotonic behavior of MET is observable in our NLH model with stochastic volatility $v(t)$ [26, 27]. This behaviour is similar to that observed for MET *versus* v in the NES effect with constant volatility v. We investigated the dynamics of the system for $c = 0$. In this case, after an exponential transient, the volatility reaches the asymptotic value b, and the NES effect is observable as a function of b. This case corresponds to the usual parametric constant volatility regime. The results are reported in Fig. 3, where MET *versus* b is plotted for three different starting unstable initial positions. The simulations were performed considering the initial positions of the process $x(t)$ in the unstable region $[x_c, x_m]$ and using an absorbing barrier at $x = -6.0$. When the "Brownian particle" $x(t)$ hits the barrier, the escape time is registered and another simulation is started, placing $x(t)$ at the same starting position x_0 and using for the volatility the value taken on at the hitting time. The nonmonotonic behavior, which is more evident for starting positions near the maximum of the potential, is always present. After the maximum, when the values of b are much greater than the potential barrier height, the exponential behavior is recovered. The results of our simulations show that the NES effect can be observed as a function of the volatility reverting level b, the effect being modulated by the parameter $(ab)/c$. The phenomenon disappears if the noise term is predominant in comparison with the reverting term: the effect is no more observable because the parameter c pushes the system towards a too noisy region. When the noise term is coupled to the reverting term, we observe the NES effect as a function of the parameter c. Finally we note that the effect disappears if b is so high as to saturate the system [27].

5. Transient dynamics of Josephson junctions

Josephson junctions (JJs) are the basis components of a great variety of supeconducting devices. They are employed in High Temperature Superconductors (HTSs), such as nanoscale Superconducting Quantum Interference Devices (SQUIDs) for the detection of very weak

magnetic fields, and in low temperatures solid state superconducting quantum bits (qubits), such as charge, flux and phase qubits [28]-[31]. In JJs, working both at high and low temperatures, the environment strongly affects the behavior of the system. In the low temperature superconductive devices it is very difficult to avoid the influence of environment that constitutes mainly a decoherence source for the system. Therefore, the study of transient dynamics of JJs in the presence of noise sources is very interesting for the understanding of the interaction between these systems and environment. The dynamics of a JJ is studied considering a fictitious Brownian particle moving in a washboard potential [32] and the behavior of the current-voltage characteristic of a JJ is strictly related to the lifetime of the superconductive metastable state of the particle. The decay of the particle from the metastable state, in fact, depends on the fluctuations of the voltage across the junction. Recently noise induced effects were experimentally observed in underdamped Josephson junctions [3, 12], and the switching to resistive state of an annular Josephson junction due to thermal activation was analyzed [33].

We present the study of the transient dynamics of short overdamped and long JJs under the influence of fluctuating bias current and oscillating potential. We numerically calculate the lifetime of the superconductive metastable state also called the mean switching time (MST) to the resistive state for short JJ (SJJ) and long JJ (LJJ). We demonstrate the presence of noise induced effects such as resonant activation (RA) [1, 2, 3, 7, 8] and noise enhanced stability (NES) [4]-[12]. We analyze both the effects of thermal and correlated noise sources. In SJJ and LJJ we consider white noise, accounting for the thermal fluctuations, and correlated (colored) noise separately. Moreover, in LJJ we present an analysis considering together the effects of white and colored noise. For given values of frequency of the driving signal and suitable noise intensity, we find maxima of the lifetime of the superconductive state. This is an interesting feature for the study of the coherence time of these devices. Our results hold for low temperature superconducting devices when we consider only the effects of the colored noise, and they can be extended to high temperatures, when both colored and white noise come into play.

5.1. Short overdamped Josephson junctions

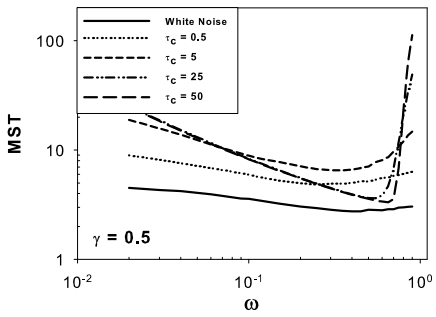

Figure 4. MST vs ω for white noise and different τ_c, γ=0.5, i_0=0.8 and A=0.7.

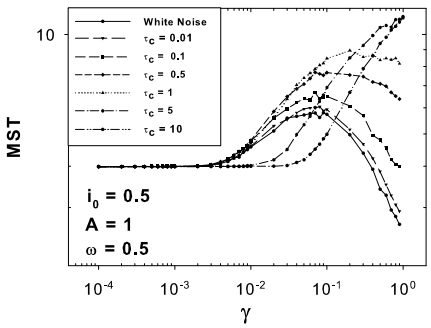

Figure 5. MST vs γ for white noise and different values of τ_c, ω=0.5, A=1, i_0=0.5.

The study of SJJs is performed in the framework of the resistive shunted junction (RSJ) model formalism [34], with a fluctuating current term. The overdamped Langevin equation to study the dynamics is [35]

$$\frac{d\phi}{dt} = -\omega_c \frac{dU(\phi)}{d\phi} - \omega_c \zeta(t), \tag{10}$$

where ϕ is the phase difference of the wave functions in the ground state between left and right superconductive sides of the junction. The characteristic frequency of the Josephson junction is $\omega_c=2eR_NI_c/\hbar$, where e is the electron charge, R_N^{-1} is the normal conductivity, I_c is the critical current and $\hbar=h/2\pi$ with h the Plank constant. In Eq. (10) the time is normalized to the inverse of the characteristic frequency of the junction ω_c. In our analysis $\zeta(t)$ is a colored noise source, generated by an Ornstein-Uhlenbeck (OU) process

$$d\zeta(t) = -\frac{1}{\tau_c}\zeta(t)dt + \frac{\sqrt{\gamma}}{\tau_c}dW(t), \tag{11}$$

where γ is the noise intensity and $W(t)$ is the Wiener process with the usual statistical properties: $\langle dW(t)\rangle = 0$, and $\langle dW(t)dW(t')\rangle = \delta(t-t')dt$. The potential profile $U(\phi)$ of Eq. (10) is given by

$$U(\phi) = 1 - cos\phi - i(t)\phi, \tag{12}$$

where $i(t) = i_0 + f(t)$, $i_0 = i_b/I_c$ is the constant dimensionless bias current and $f(t)=Asin\omega t$ is the driving current with dimensionless amplitude $A = i_s/I_c$ and frequency ω (i_b and i_s represent the bias current and the driving current amplitude respectively). We investigate the dynamics of the Brownian particle in the presence of a time-dependent nonlinear periodic potential, by solving numerically Eq. (10), for ω_c=1. To study the lifetime of the superconductive state we take, as initial condition for the particle, the minimum of the potential profile, corresponding to the condition $\phi_0=arcsin(i_0)$ and we calculate the time spent by the particle to reach the next maximum. In Fig. 4 we report the behavior of MST vs ω, for the noise intensity $\gamma = 0.5$, and different values of τ_c. The non-monotonic behavior of the curves shows that the RA phenomenon, already found in the presence of white noise [8, 35], appears also with colored noise. The values of MST around the minimum are influenced by the variation of τ_c. Moreover, we find, in a wide range of frequency ($0.3 < \omega < 0.8$) (see Fig. 4), a non-monotonic behavior of MST as a function of the correlation time.

In Fig. 5, we show the behavior of MST as a function of the noise intensity for different values of the correlation time. We note the appearance of noise enhanced stability (NES), a phenomenon already found in short JJs in the presence of white noise [8, 35]. Here we observe a range of values of correlation time, namely $0.01<\tau_c<1$, in which the curves present a non-monotonic behavior. For τ_c=5,10, the non-monotonic behavior disappears.

5.2. Long Josephson junctions

The investigation of LJJs is developed in the framework of the sine-Gordon model [34, 36]. The dynamics of a LJJ is described by the motion of a phase string in a one dimensional washboard potential. The transient dynamics is represented by a nonlinear partial differential equation with a stochastic term [37, 38]

$$\beta\frac{\partial^2\phi}{\partial t^2} + \frac{\partial\phi}{\partial t} + \frac{\partial^2\phi}{\partial x^2} = i(x) - \sin\phi + i_f(x,t), \tag{13}$$

where $\beta = \omega_c RC$, with R and C the LJJ equivalent resistance and capacitance, respectively. Here $i(x)$ and $i_f(x,t)$ are the bias current density and the fluctuating current density normalized to the critical current density I_c of the junction, respectively. In Eq. (13) time is normalized to the inverse of the characteristic frequency, $\omega_c = 2eRI_c/\hbar$, of the junction. Analogously length is normalized to the Josephson penetration depth (λ_J). The boundary conditions for Eq. (13) are:

$$\frac{\partial\phi(0,t)}{\partial x} = \frac{\partial\phi(L,t)}{\partial x} = 0. \tag{14}$$

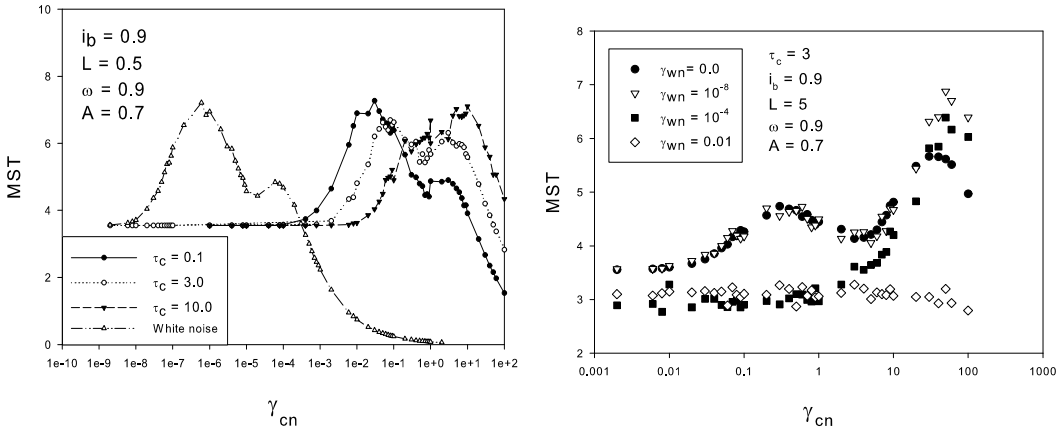

Figure 6. Left panel: MST vs γ_{cn} with $i_b = 0.9$ and L=0.5. Right panel: MST vs γ_{cn} with $i_b = 0.9$ and L=5, for different values of white noise intensity.

where $L = l/\lambda_J$ with l the length of the junction. As initial position of the phase string in the washboard potential, we consider the minimum, represented by the condition $\phi(x,0) = arcsin(i_b)$. We studied, first, the effects of a fluctuating current signal described by a correlated noise and, then, the effects of both colored and white noise on the system, by inserting in Eq. (13) a fluctuating term given by the sum of a correlated noisy current signal, $i_{cn}(x,t)$, and a thermal current signal, $i_{wn}(x,t)$, namely $i_f(x,t) = i_{cn}(x,t) + i_{wn}(x,t)$. In the presence of colored noise we found the noise induced effects such as RA and NES. In particular in left panel of Fig. 6 the non-monotonic behavior of MST as a function of the noise intensity γ_{cn} indicates the presence of the NES effect. The maxima of the curves depend by different values of τ_c. The effects of both colored and white noise are presented in right panel of Fig. 6, where the curves of MST vs γ_{cn} are calculated for different white noise intensities γ_{wn}, with $L = 5$. We note that when γ_{wn} is greater than γ_{cn} the effects of colored noise disappear. If we consider γ_{wn} suitably lower than γ_{cn}, the effects of colored noise become evident. In fact, when γ_{cn} is at least five order of magnitude higher than γ_{wn}, the curve of MST vs γ_{cn} (empty triangles) matches with good agreement that (black circles) obtained in the absence of white noise (see right panel of Fig. 6 for γ_{wn}=10^{-8}).

6. Metastability in a quantum system

Quantum tunneling effect occurs often in condensed matter physics, examples are JJs, hetero-nanostructures, etc.. The tunneling effect plays an important role in the nonlinear relaxation time from a metastable state in an open quantum system, interacting with a thermal bath. Symmetrical and asymmetric bistable systems are good quantum model systems for analysis of the "superconducting quantum bits" and decoherence phenomena. To obtain very long coherence times in the presence of interaction between the qubit and the noisy environment is one of the greatest challenges of physics. The influence of the environment in quantum tunneling has been in the focus of intense research over the last years [39]-[42]. The environment is commonly described as an ensemble of harmonic oscillators (thermal bath) at thermal equilibrium at temperature T, with a bilinear coupling between the quantum system and the thermal bath. By this kind of coupling between system and environment the quantum mechanical analogue of the generalized Langevin equation can be derived [39]. Time-dependent driving fields, such as laser beams, have most interesting implications for quantum systems. These time-dependent fields give rise to interesting effects, such as the coherent destruction of tunneling [43], the effect of quantum stochastic resonance [44], and the control and reduction of decoherence in open

quantum systems [45]. In this work we analyze a time-dependent asynmmetric bistable potential by using the approach of the Feynman-Vernon functional [46] in discrete variable representation (DVR) [47, 48].

6.1. The model

The starting point of our investigation is the Caldeira-Leggett model [39] for a quantum particle with mass M interacting with a thermal bath. The particle, with position operator $\mathbf{q}$ and momentum operator $\mathbf{p}$ is moving in an asymmetric one-dimensional double-well potential V_0 ($\mathbf{q}$) in the presence of a time-dependent external force, $A\sin(\Omega t)$. The unperturbed Hamiltonian of the system is

$$\mathbf{H}_u n(t) \quad = \quad \frac{\mathbf{p}^2}{2M} + V_0(\mathbf{q}) - A\sin(\Omega t), \tag{15}$$

and the potential is

$$V_0(\mathbf{q}) = \frac{M^2\omega_0^4}{64\Delta U}\mathbf{q}^4 - \frac{M\omega_0^4}{4}\mathbf{q}^2 - \mathbf{q}\epsilon, \tag{16}$$

where ϵ is the asymmetry parameter. The environment is modelled [39] as an ensemble of harmonic oscillators

$$\mathbf{H}_B = \sum_{j=1}^{\mathcal{N}} \frac{1}{2}\left[\frac{\mathbf{p}_j^2}{m_j} + m_j\omega_j^2\left(\mathbf{x}_j - \frac{c_j}{m_j\omega_j^2}\mathbf{q}\right)^2\right]. \tag{17}$$

The full Hamiltonian (system + bath) is $\mathbf{H}(t) = \mathbf{H}_u n(t) + \mathbf{H}_B$. As $\mathcal{N} \to \infty$, in Eq. (17), we have a continuous spectral density. We use an Ohmic spectral density with an exponential cut-off $J(\omega) = \eta\omega\exp\left(\frac{\omega}{\omega_c}\right)$. Because of the bilinear coupling between the coordinate $\mathbf{q}$ of the system and the coordinate $\mathbf{x}$ of thermal bath we can consider this as a quantum analogue of the multiplicative noise in classical systems.

By following the Feynman-Vernon approach [46] the reduced density operator can be written as

$$\rho(q_f, q_f'; t) = \int dq_0 \int dq_0' K(q_f, q_f', t; q_0, q_0', t_0)\rho_S(q_0, q_0', t_0), \tag{18}$$

where the propagator K is given by

$$K(q_f, q_f', t; q_0, q_0', t_0) = \int_{q(t_0)=q_0}^{q(t)=q_f} \mathcal{D}q \int_{q'(t_0)=q_0'}^{q'(t)=q_f'} \mathcal{D}q' \mathcal{A}[q]\mathcal{A}^*[q']\mathcal{F}_{FV}[q, q'], \tag{19}$$

and $\mathcal{A}[q] = \exp\left(\frac{iS_S[q]}{\hbar}\right)$ with $S_S[q]$ being the classical action functional. In Eq. (19) $\mathcal{F}_{FV}[q, q'] = \exp\left(\frac{-\phi_{FV}[q,q']}{\hbar}\right)$ is the Feynman Vernon influence functional, which depends on the bath correlation function [41].

6.2. Discrete variable representation

By using the discrete variable representation (DVR) [47], with the discrete eigenbasis of the position operator $\mathbf{q}$, and the generalized non-interacting cluster approximation [48] it is possible to obtain a generalized Master Equation (GME)

$$\rho_{\mu\mu}(t) = \sum_{\nu=1}^{M} \int_{t_0}^{t} dt' H_{\mu\nu}(t - t')\rho_{\nu\nu}(t') + I_\mu(t - t_0), \quad \mu = 1, \ldots, M \ , \tag{20}$$

neglecting all the intercluster interactions and taking into account the paths that start in an off-diagonal element (see Ref. [48] for details). Since the inhomogeneities $I_\mu(t, t_0)$ do not contribute

to the long-time dynamics because decay exponentially with time on a rather short time scale, this term can be neglected. We assume furthermore that the characteristic memory time τ_{mem} of the kernels of Eq. (20) is the smallest time scale of the problem (*Markovian limit*). This means that we can substitute the argument of $\rho_{\nu\nu}(t')$ under the integral by the time t and draw $\rho_{\nu\nu}(t)$ in front of the integral. We then obtain the *Markovian approximated generalized master equation*

$$\dot{\rho}_{\mu\mu}(t) = \sum_{\nu=1}^{M} \Gamma_{\mu\nu}(t)\rho_{\nu\nu}(t), \tag{21}$$

with the time-dependent rate coefficients

$$\Gamma_{\mu\nu}(t) = \int_0^\infty d\tau H_{\mu\nu}(t, t-\tau). \tag{22}$$

Since the diagonal elements $\rho_{\mu\mu}(t)$ obey Eq. (21), the long-time dynamics in this regime is ruled by a single exponential decay. Thus the Eq. (21) is a set of coupled ordinary first-order differential equations, which can be decoupled via a diagonalization procedure. The diagonalized rate matrix reads

$$\sum_{\kappa_1,\kappa_2=1}^{M} (S^{-1})_{\mu\kappa_1}\Gamma_{\kappa_1\kappa_2}S_{\kappa_2\nu} = \Lambda_\mu\delta_{\mu\nu}, \tag{23}$$

where $S_{\mu\nu}$ denotes the element of the transformation matrix and Λ_μ the eigenvalues of the rate matrix. The general solution of the Markov approximated GME is

$$\rho_{\mu\mu}(t) = \sum_{\nu,\kappa=1}^{M} S_{\mu\nu}(S^{-1})_{\mu\kappa}e^{\Lambda_\nu(t-t_0)}\rho_{\kappa\kappa}(t_0). \tag{24}$$

Since the diagonal elements of the rate matrix are the negative sum of the matrix elements of the corresponding columns, one eigenvalue equals to zero, i.e., $\Lambda_1 = 0$. Therefore,

$$\rho_{\mu\mu}(t) = \rho^{\infty}_{\mu\mu} + \sum_{\nu=2}^{M}\sum_{\kappa=1}^{M} S_{\mu\nu}(S^{-1})_{\mu\kappa}e^{\Lambda_\nu(t-t_0)}\rho_{\kappa\kappa}(t_0). \tag{25}$$

with $\rho^{\infty}_{\mu\mu} = \sum_{\kappa=1}^{M} S_{\mu,1}(S^{-1})_{1,\kappa}\rho_{\kappa\kappa}(t_0)$ being the asymptotic population of the DVR-state $\mid q_\mu >$. The rate which determines the dynamics on the largest time-scale is the smallest non-zero absolute value of the real part of the eigenvalues of the rate matrix, i.e. *the quantum relaxation rate*

$$\Gamma \equiv \min\{\mid Re\Lambda_\nu \mid; \nu = 2, \ldots, M\}. \tag{26}$$

6.3. Results

In Fig. 7 we report the first four global states $< q \mid \psi_1 >, \ldots, < q \mid \psi_4 >$ for barrier height $E_B = \Delta U/\hbar\omega_0 = 1.4$ and asymmetry parameter $\varepsilon = 0.23$. The corresponding potential profile has a metastable state on the left well. The quantum relaxation rate Γ as a function of the asymmetry parameter is reported in Fig. 8 for different temperatures. There are many overlapping regions where is visible a nonmonotonic behaviour of Γ as a function of the temperature. We can distinguish two different nonmonotonic behaviours: one with a maximum, reported in Fig. 9, and the other one with a minimum. This last one corresponds to the noise enhanced stability effect revealed in classical metastable systems, that is a noise enhanced stability quantum effect.

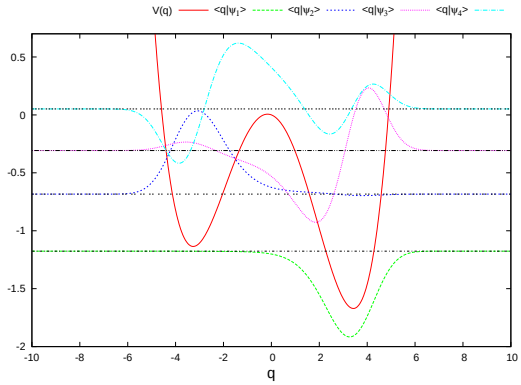

Figure 7. The first four global states $< q \mid \psi_1 >, \ldots, < q \mid \psi_4 >$ for barrier height $E_B = \Delta U/\hbar\omega_0 = 1.4$ and bias $\varepsilon = 0.23$.

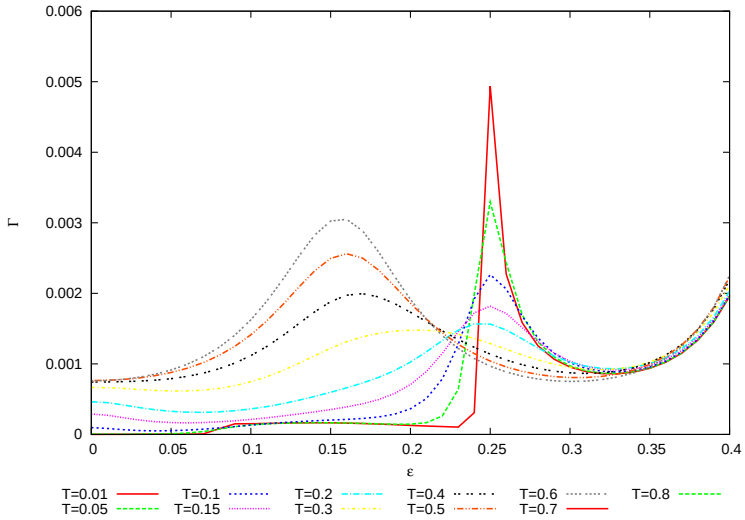

Figure 8. Quantum relaxation rate Γ as a function of the asymmetry parameter ε for different temperatures T. The barrier height is $E_B = 1.4$ and the number of energy levels is $M = 4$.The bath parameters are $\eta = 0.1$ and $\omega_c = 10.0$.

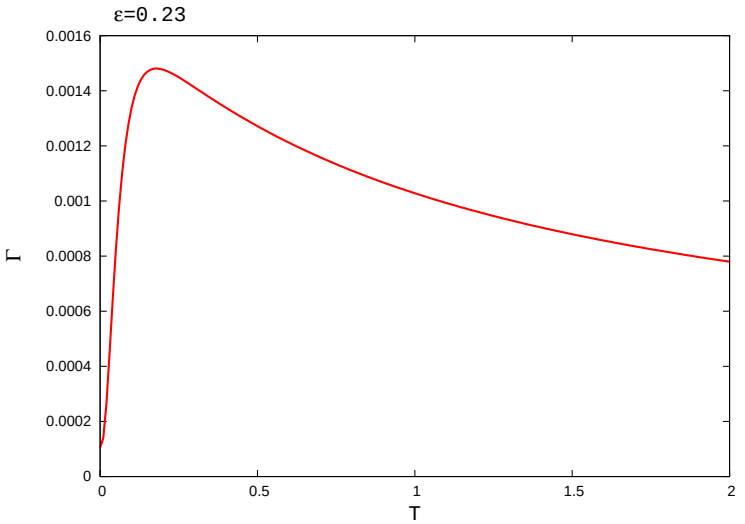

Figure 9. Quantum relaxation rate Γ as a function of the temperature T for fixed asymmetric parameter $\epsilon = 0.23$. The barrier height is $E_B = 1.4$ and the number of energy levels is $M = 4$.The bath parameters are $\eta = 0.1$ and $\omega_c = 10.0$.

Acknowledgments
This work was supported by MIUR.

References
[1] Doering C R and Gadoua J A 1992 *Phys. Rev. Lett.* **69** 2318
[2] Mantegna R N and Spagnolo B 2000 *Phys. Rev. Lett.* **84** 3025
[3] Yu Y and Han S 2003 *Phys. Rev. Lett.* **91** 127003
[4] Mantegna R N and Spagnolo B 1996 *Phys. Rev. Lett.* **76** 563
[5] Mielke A 2000 *Phys. Rev. Lett.* **84** 818.
[6] Agudov N V and Spagnolo B 2001 *Phys. Rev.* E **64**, 035102(R)
[7] Dubkov A A, Agudov N V and Spagnolo B 2004 *Phys. Rev.* E **69** 061103
[8] Pankratov A L and Spagnolo B 2004 *Phys. Rev. Lett.* **93** 177001
[9] Fiasconaro A, Spagnolo B and Boccaletti S 2005 *Phys. Rev.* E **72** 061110(5)
[10] Hurtado P I, Marro J and Garrido P L 2006 *Phys. Rev.* E **74** 050101(R)
[11] Spagnolo B, Dubkov A A, Pankratov A L, Pankratova E V, Fiasconaro A and Ochab-Marcinek A 2007 *Acta Physica Polonica* B **38** 1925
[12] Sun G *et al* 2007 *Phys. Rev.* E **75** 021107(4)
[13] Kasianowicz J J, Brandin E, Branton D and Deamer D W 1996 *Proc. Natl. Acad. Sci. USA* **93** 13770
[14] Meller A and Branton D 2002 *Electrophoresis* **23** 2583.
[15] Han J, Turner S W and Craighead H G 1999 *Phys. Rev. Lett.* **83** 1688
[16] Pizzolato N, Fiasconaro A and Spagnolo B 2008 *Int. J. Bif. Chaos* **18** 2871
[17] Pizzolato N, Fiasconaro A and Spagnolo B 2009 *J. Stat. Mech.* **P01011**
[18] Valenti D, Augello G and Spagnolo B 2008 *Eur. Phys. J.* B **65** 443
[19] Pankratova E V, Polovinkin A V and Spagnolo B 2005 *Phys. Lett. A* **344** 43
[20] Mantegna R N and Stanley H E 2000 *An Introduction to Econophysics: Correlations and Complexity in Finance* (Cambridge, UK: Cambridge U. Press)
[21] Bouchaud J P and Potters M 2004 *Theory of Financial Risks and Derivative Pricing* (Cambridge, UK: Cambridge U. Press)
[22] Drăgulescu A A and Yakovenko V M 2002 *Quantitative Finance* **2** 443
[23] Miccichè S, Bonanno G, Lillo F and Mantegna R N 2002 *Physica* A **314** 756
[24] Silva A C, Prange R E and Yakovenko V M 2004 *Physica* A **344** 227
[25] Bonanno G and Spagnolo B 2005 *Fluc. Noise Lett.* **5**, L325
[26] Bonanno G, Valenti D and Spagnolo B 2006 *Eur. Phys. J.* B **53** 405
[27] Bonanno G, Valenti D and Spagnolo B 2007 *Phys. Rev.* E **75** 016106
[28] Wu C H *et al* 2008 *Nanotechnology* **19** 315304
[29] Nakamura Y *et al* 1999 *Nature* **398** 786
[30] Friedman J R *et al* 2000 *Nature* **406** 43
[31] Martinis J M *et al* 2002 *Phys. Rev. Lett.* **89** 117901
[32] Yu Y *et al* 2002 *Science* **296** 889
[33] Gulevich D and Kusmartsev F2006 *Physica* C **435** 87
[34] Barone A and Paternò G 1982 *Physics and Application of the Josephson Effect* (New York: Wiley) 122
[35] Gordeeva A V *et al* 2008 *Int. J. Bif. Chaos* **18** 2823.
[36] Gulevich D R *et al* 2008 *Phys. Rev. Lett.* **101** 127002
[37] Fedorov K G and Pankratov A 2007 *Phys. Rev.* B **76** 024504
[38] Fedorov K G, Pankratov A L and Spagnolo B 2008 *Int. J. Bif. Chaos* **18** 2855
[39] Caldeira A O and Leggett A L 1981 *Phys. Rev. Lett.* **46** 211
[40] Leggett A J, Chakravarty S, Dorsey A T, Fisher M, Garg A and Zwerger W 1987 *Rev. Mod. Phys.* **59** 1
[41] Weiss U 1999 *Quantum Dissipative Systems* (Singapore: World Scientific)
[42] Grifoni M and Hänggi P 1998 *Phys. Rep.* **304** 230
[43] Grossmann F, Dittrich T, Jung P and Hänggi P 1991 *Phys. Rev. Lett.* **67** 516
[44] Löfstedt R and Coppersmith S. N. 1994 *Phys. Rev. Lett.* **72** 1947.
[45] Viola L, Knill E and Lloyd S 1999 *Phys. Rev. Lett.* **82** 2417
[46] Feynman R P and Vernon F L, Jr. 1963 *Ann. Phys. (N.Y.)* **24** 118
[47] Harris D O, Engerholm G G and Gwinn W D 1965 *J. Chem. Phys.* **43** 1515
[48] Thorwart M, Grifoni M and Hänggi P 2001 *Annals of Physics* **293** 15